SUPPLEMENTARY INFORMATION

Amphiphilic electrospun scaffolds of PLLA-PEO-PPO block copolymers: preparation, characterization and drug-release behaviour

Lívia M. D. Loiola[†], Pablo R. Cortez Tornello[‡], Gustavo A. Abraham[‡], Maria I. Felisberti[†]

[†]Institute of Chemistry, University of Campinas – UNICAMP, P.O. Box 6154, 13083-970, Campinas, São Paulo, Brazil.

[‡]Research Institute of Materials Science and Technology, INTEMA (UNMdP - CONICET), Av. J. B. Justo 4302, B7608FDQ, Mar del Plata, Argentina.

PELA and PEPELA amphiphilic block copolymers were synthesized by ring-opening polymerization of LLA in a coordination-insertion mechanism from diol PEO and PEO-*b*-PPO-*b*-PEO polyether macroinitiators using $Sn(Oct)_2$ as catalyst. The equimolar $Sn(Oct)_2$/hydroxyl groups ratio ($n_{catalyst}$:$n_{macroinitiator}$ = 2:1) was used to produce high molar mass block copolymers and large yields (79-91%). [(1), (2), (3)]

Considering symmetrical PLLA block insertions during synthesis, ^{1}H NMR spectra (Figure S1) were used to determine the degree of polymerization of PLLA and hence the overall PELA and PEPELA copolymer molar masses (Table 1), calculated from the integration of specific signals at δ = 5.2 ppm (-C*H*(CH_3)COO-) for PLLA blocks and at δ = 3.6 ppm (-CH_2CH_2-O-) for PEO blocks, and applying the previously calculated molar masses from the esterified macroinitiators (Table 1). [(4)] The ratio between the number of LLA units and the total number of EO and PO repeating units in the copolymers

(n_{LLA}/n_{EO+PO}) was also determined by ^{1}H NMR, and the values were similar to those obtained for the reaction medium (Table 1). [4–6]

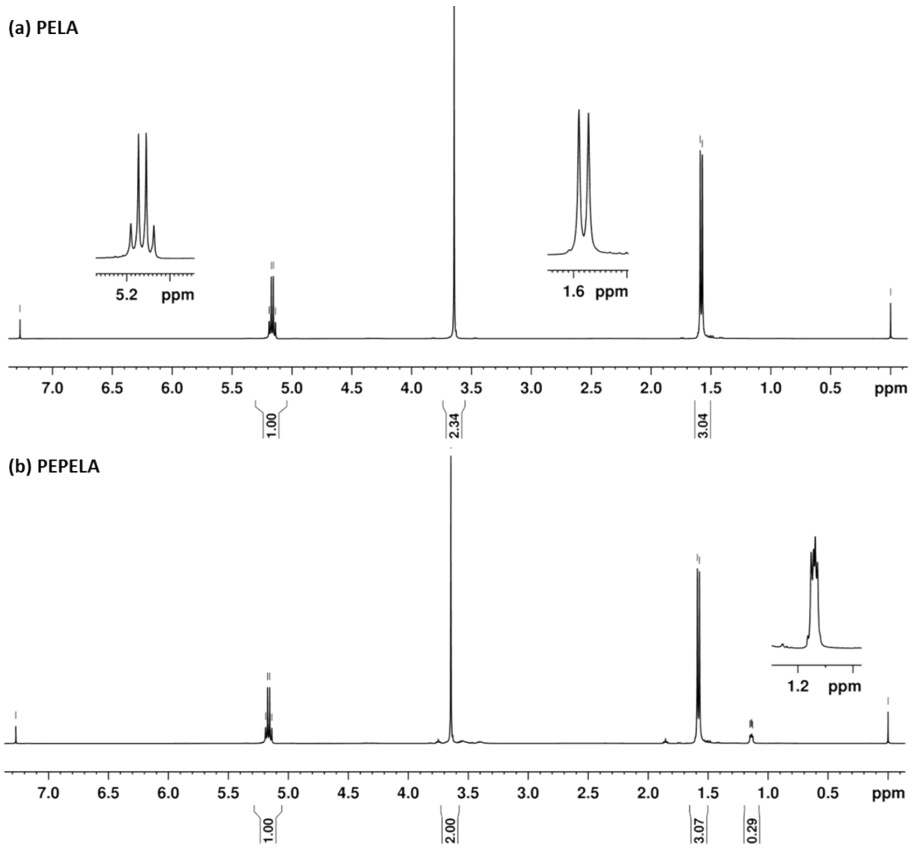

Figure S1: ^{1}H NMR spectra of PELA (a) and PEPELA (b) copolymers. The characteristic peaks at approximately 5.2 ppm (1H, *q*) and 1.6 ppm (3H, *d*) are assigned to the methine (-CH) and methyl (-CH_3) protons of the LLA units, respectively; the peak at the 3.6 ppm (2H, *s*) is assigned to the methylene protons (-CH_2) of the EO units, and the peak at the 1.1 ppm (3H, *m*) is assigned to the methyl protons (-CH_3) of the PO units.

GPC analysis of PELA and PEPELA amphiphilic copolymers (Figure S2) provide number-average molar masses (M_n) relative to the PS standards used for calibration. Because of this, the values calculated by ^{1}H NMR are preferable. The polydispersity index (M_w/M_n) obtained from GPC data (Table 1) represent the molar mass distribution of polymers independent of the nature of the standards used for calibration.

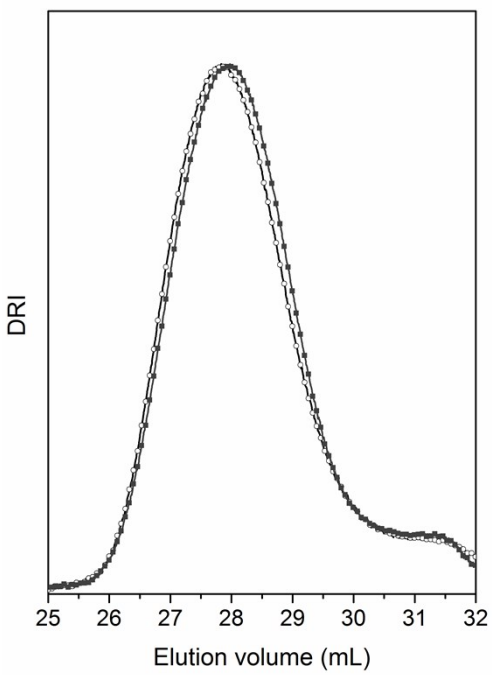

Figure S2: Chromatogram from GPC analysis of the PELA (○) and PEPELA (■) copolymers directly after synthesis (before electrospinning processing).

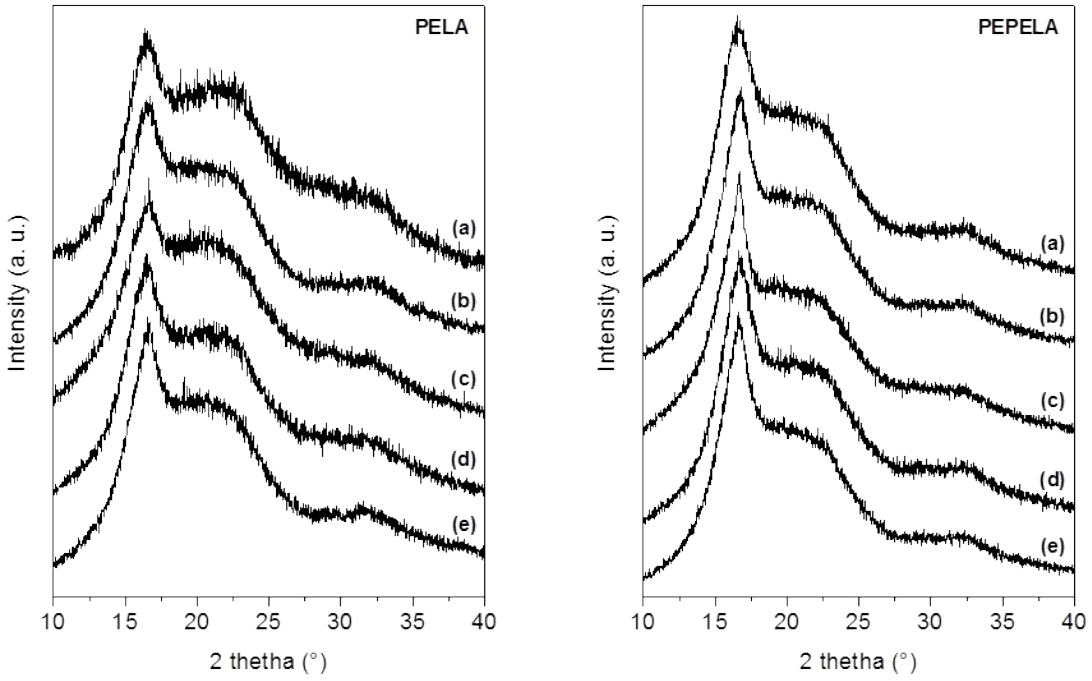

Figure S3: XRD patterns of PELA and PEPELA scaffolds without drugs (a), loaded with 2.5 wt.% (b) and 5 wt.% (c) of acetaminophen, and loaded with 2.5 wt.% (d) and 5 wt.% (e) of celecoxib.

The addition of AC or CL drugs to PELA and PEPELA results in changes in the fibre diameter, and in number, size and shape of the beads of the scaffolds - Table 2 and Figure S4:

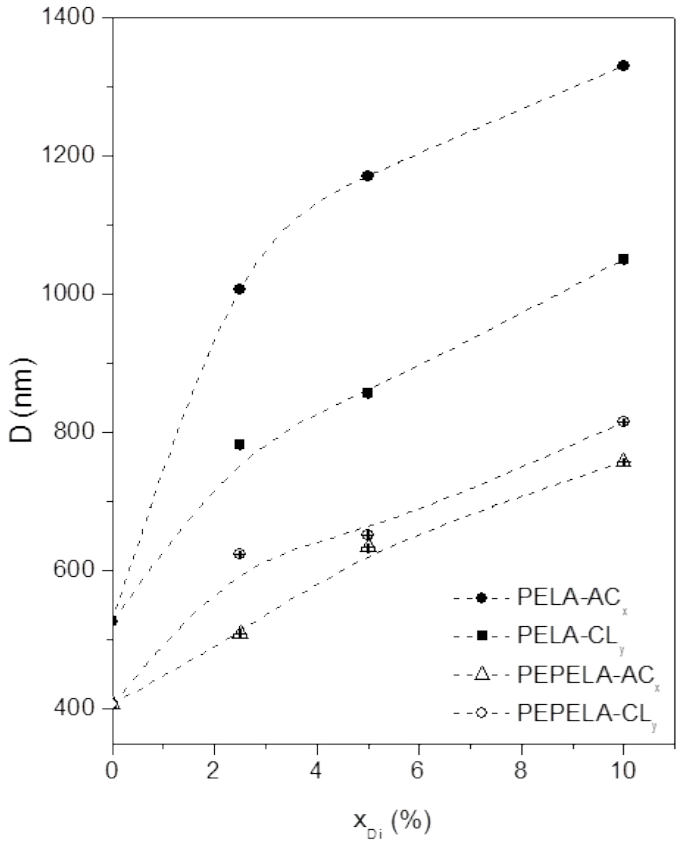

Figure S4: Mean fibre diameter (*D*) as a function of the initial mass fraction of the drug in the spinning solutions (x_{Di}) for (℘) PELA-AC_x, (O) PELA-CL_y, (❒) PEPELA-AC_x and (∾) PEPELA-CL_y series.

Under DSC cooling, PLLA phase of the copolymers in the neat and loaded scaffolds partially crystallized, which is depicted by exothermic peaks at approximately T_c = 90°C. The partially crystallized PLLA copolymer phase undergoes further cold crystallization at approximately 100°C only for PELA-AC_{10}, PEPELA-AC_5 and PEPELA-AC_{10} scaffolds

during the subsequent DSC 2nd heating scan. Also in the 2nd heating curves, PELA and PEPELA neat and loaded scaffolds present glass transition at approximately -15°C, referring to the polyether phase. In some cases, the polyether phase of the scaffolds was capable to crystallize, and a low intensity melting peak at approximately 35°C was observed for the scaffolds, with the exception of loaded PEPELA. Melting temperature at approximately 160°C and melting enthalpy of PLLA phase of all scaffolds did not vary significantly.

Besides the drug effect, the electrospinning process also influences the crystallization of the copolymer, since the polymer chains are elongated by the applied electric field along the solution jet direction and quenched upon rapid solvent evaporation, which restricts the chain segments mobility, folding and consequently reduces the degree of crystallization. [7]

The molten liquids were held at high temperatures (200°C) ensuring the elimination of all crystals, and they did not crystallize upon the cooling step at 20°C min^{-1}, remaining as amorphous drugs. As the amorphous AC sample is heated again, it presents a glass transition at 30°C and then two exothermic peaks, referring to the AC amorphous-to-type III transition ($T_{a\text{-}III,onset}$ = 80°C) and type III-to-type II transition ($T_{III\text{-}II,onset}$ = 127°C), followed by the melting at $T_{m,\ onset}$ = 159°C of the polymorphic mixture of AC. [8], [9] The amorphous CL presents in the 2nd heating a glass transition at 64°C, followed by an exothermic peak ($T_{cc,onset}$ = 133°C) and an endothermic peak ($T_{m,onset}$ = 162°C), referring to the cold crystallization and melting of CL. [10], [11]

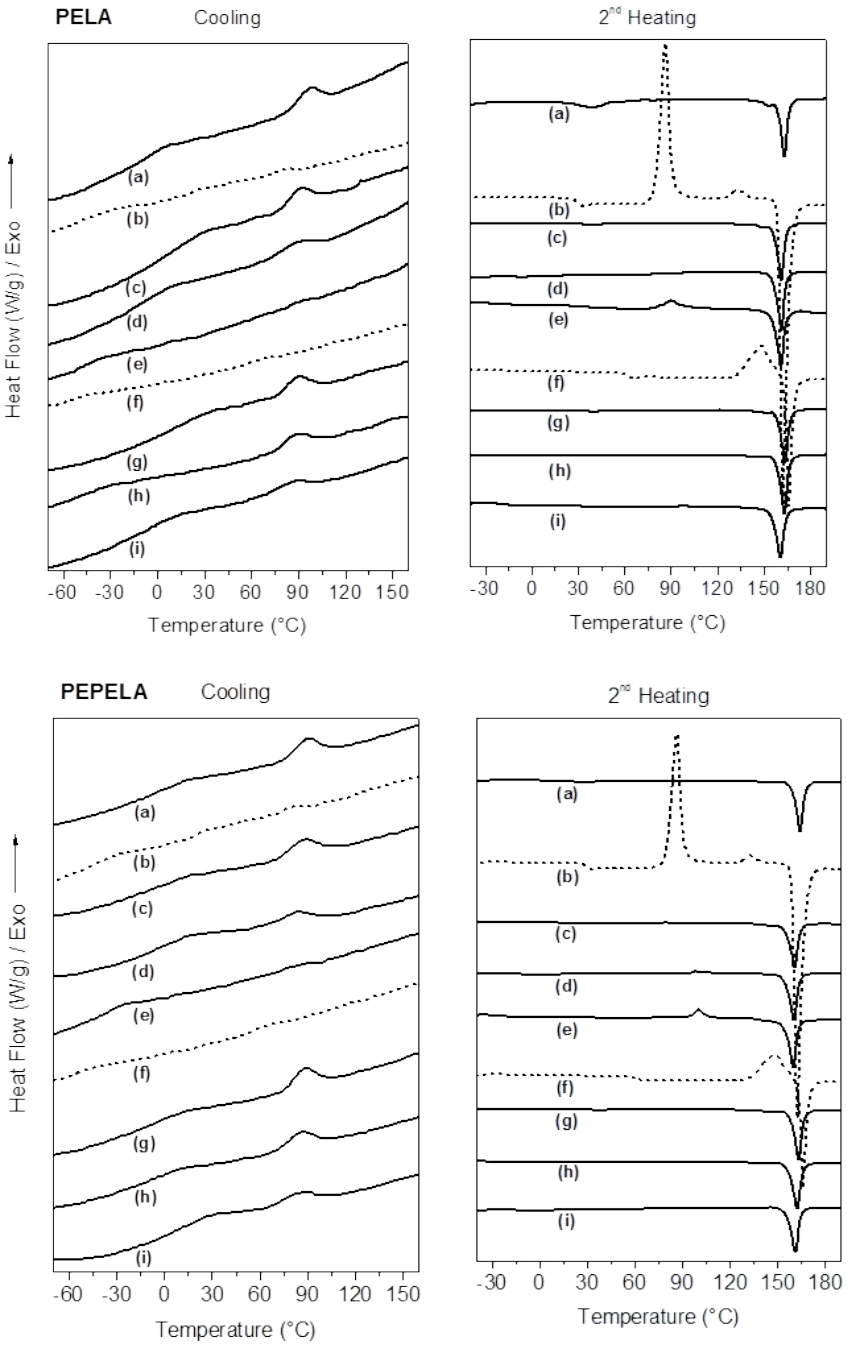

Figure S5: DSC cooling and 2nd heating curves at 20°C/min for PELA and PEPELA scaffolds: (a) without drug, (b) acetaminophen and acetaminophen-loaded scaffolds (c) $AC_{2.5}$, (d) AC_5, (e) AC_{10}; (f) celecoxib and celecoxib-loaded scaffolds (g) $CL_{2.5}$, (h) CL_5, (i) CL_{10}.

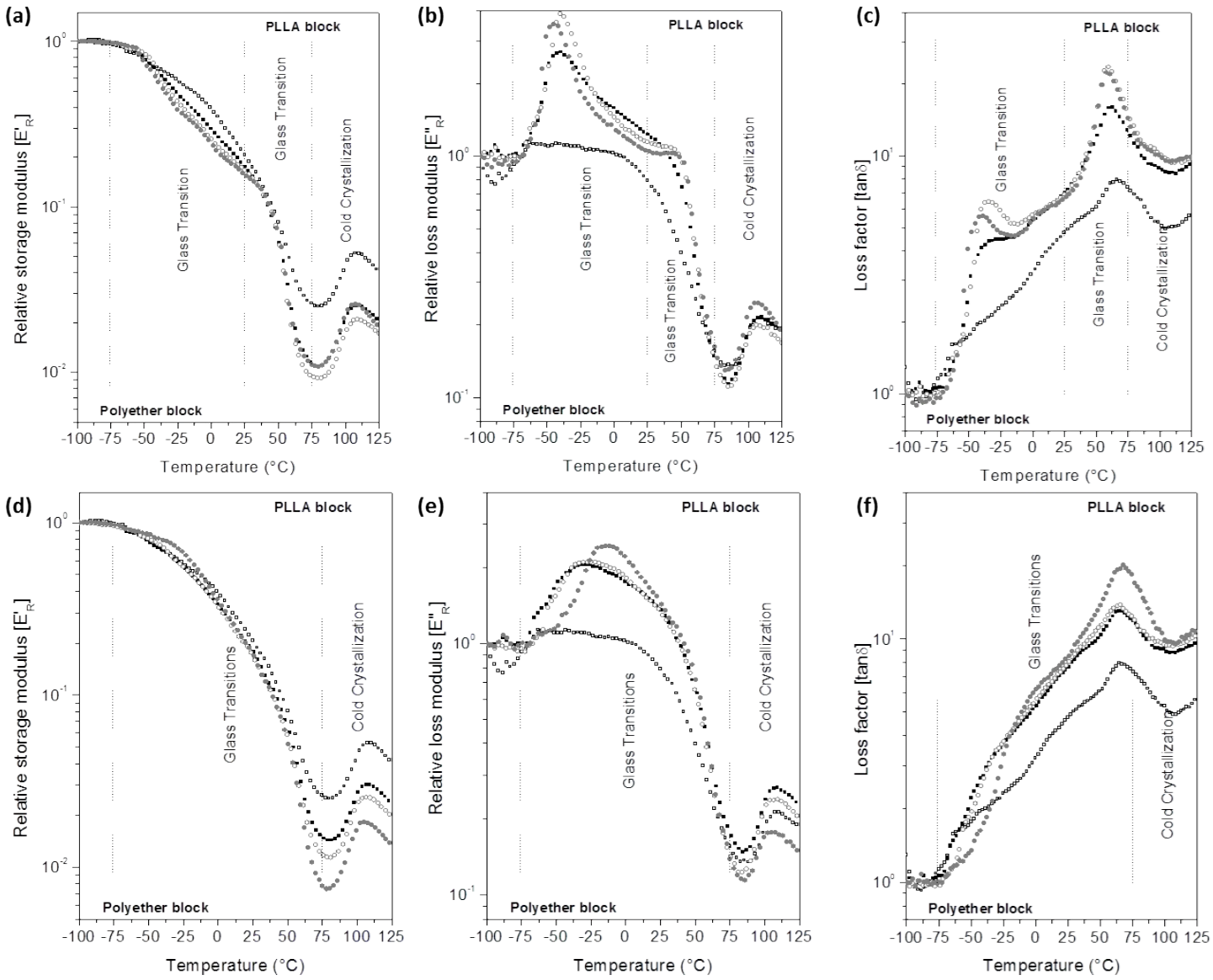

Figure S6: Relative storage (E'_R) and loss (E''_R) moduli and loss factor (tanδ) as a function of temperature for PEPELA scaffolds loaded with acetaminophen (a, b, c) or celecoxib (d, e, f) drugs at concentrations of 0.0 (□), 2.5 (■), 5.0 (○) and 10 wt.% (●) of initial drug load.

Table S1: Thermal properties of AC and CL drugs and PELA-AC_x, PELA-CL_y, PEPELA-AC_x and PEPELA-CL_y scaffolds, as determined by DSC and DMA.

Material	***DSC 1st Heating***								***Cooling***		***2nd Heating***							***DMA***	
	T_g^i /°C	T_g^{ii} /°C	T_m^i /°C	ΔH_m^i /Jg^{-1}	T_c^{ii} /°C	ΔH_c^{ii} /Jg^{-1}	T_m^{ii} /°C	ΔH_m^{ii} /Jg^{-1}	T_c^{ii} /°C	ΔH_c^{ii} /Jg^{-1}	T_g^i /°C	T_c^{ii} /°C	ΔH_c^{ii} /Jg^{-1}	T_m^i /°C	ΔH_m^i /Jg^{-1}	T_m^{ii} /°C	ΔH_m^{ii} /Jg^{-1}	T_g^i /°C	T_g^{ii} /°C
AC[iii]	-	-	-	-	-	-	171	187	-	-	30	80 127	112 7.5	-	-	159	174	-	-
CL[iii]	-	-	-	-	-	-	162	95	-	-	64	133	49	-	-	162	51	-	-
PELA	-	52	-	-	98	19	163	49	95	27	-10	-	-	39	35	163	47	-43	37
PELA-$AC_{2.5}$	-10	46	-	-	96	19	162	43	88	28	-11	-	-	39	5.5	161	46	-45	39
PELA-AC_5	-13	42	54	8.7	93	15	162	46	94	-	-9	99	1.1	-	-	161	49	-47	50
PELA-AC_{10}	-	-	56	14	94	15	162	45	-	0	-19	90	14	-	-	161	47	-43	51
PELA-$CL_{2.5}$	-11	50	68	4.2	97	16	164	43	88	22	-13	-	-	39	3.3	164	43	-13 *broad*	
PELA-CL_5	-14	57	-	-	96	19	163	42	86	15	-11	-	-	-	-	163	45	-21 *broad*	
PELA-CL_{10}	-14	45	62	5.9	96	16	161	45	90	-	-18	96	1.2	-	-	161	47	-24 *broad*	
PEPELA	-	60	-	-	98	19	164	47	88	34	-9	-	-	29	8.1	164	47	-28 *broad*	
PEPELA-$AC_{2.5}$	-	47	-	-	95	18	162	49	84	28	-13	-	-	-	-	161	49	-40	42
PEPELA-AC_5	-10	35	53	7.3	95	16	161	47	79	10	-18	98	3.4	-	-	160	49	-41	45
PEPELA-AC_{10}	-	53	-	-	96	13	161	46	-	-	-18	100	10	-	-	160	49	-44	47
PEPELA-$CL_{2.5}$	-	59	-	-	97	18	163	47	87	25	-18	-	-	-	-	163	46	-13 *broad*	
PEPELA-CL_5	-10	59	-	-	95	16	163	47	86	32	-13	-	-	-	-	162	48	-27 *broad*	
PEPELA-CL_{10}	-11	57	-	-	95	14	161	45	87	26	-14	-	-	-	-	161	47	-14 *broad*	

[i]Transition referring to the polyether (PEO or PEO-*b*-PPO-*b*-PEO) phase in PELA and PEPELA scaffolds.

[ii]Transition referring to the polyester PLLA phase in PELA and PEPELA scaffolds.

ΔH^i and ΔH^{ii} were calculated, respectively related to polyether and PLLA phase mass.

[iii]T_{onset} for the chemically defined substances AC e CL.

AC spectrum exhibits the characteristic Raman shifts at 1650 (C=O stretching - $\nu_{C=O}$), 1620 (N-H bending - δ_{N-H}), 1560 ($\nu_{H-N-C=O}$), 1321 (δ_{C-H}), and the exclusive of AC type I 1236 (ν_{C-N}) and 835 cm^{-1} (δ_{C-H} out of the plane) [(9), (12)], while the CL type III characteristic peaks are at 3234 and 1551 cm^{-1} (respectively ν_{N-H} and δ_{N-H} in sulfonamides), 1345 and 1161 cm^{-1} ($\nu_{S=O}$), 1276 and 1228 cm^{-1} (ν_{C-F}). [(10), (11)] Unloaded PELA and PEPELA scaffold spectra present similar Raman shifts at 3002, 2946 and 2880 cm^{-1} (ν_{C-H}); 1765 cm^{-1} ($\nu_{C=O}$), 1452 and 1295 cm^{-1} (δ_{C-H}); 1130, 1090 and 1042 cm^{-1} (ν_{C-C} and ν_{C-O}). [(13–16)]

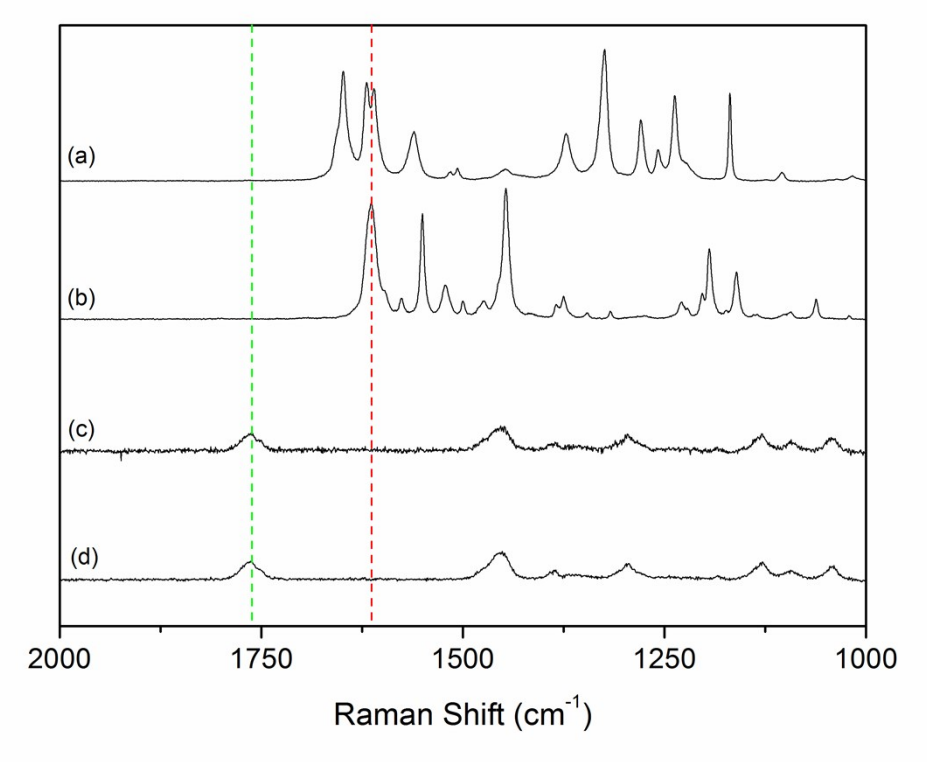

Figure S7: Full-range Raman spectra for acetaminophen (a) and celecoxib (b), and the unloaded PELA (c) and PEPELA (d) scaffolds. The green line depicts the copolymers' selected peak in the Raman shift range of 1765-1766 cm^{-1}. The red line corresponds to selected range of 1619-1620 cm^{-1} for AC and of 1618-1619 cm^{-1} for CL.

REFERENCES

1. Kricheldorf HR. Syntheses and application of polylactides. Chemosphere [Internet]. 2001 Apr;43(1):49–54. Available from: http://www.ncbi.nlm.nih.gov/pubmed/11233824

2. Trinca RB, Felisberti MI. Influence of the synthesis conditions on the structural and thermal properties of poly(l -lactide)- b -poly(ethylene glycol)- b -poly(l -lactide). J Appl Polym Sci [Internet]. 2014 Jul 5 [cited 2014 May 11];131(13):40419. Available from: http://doi.wiley.com/10.1002/app.40419

3. Loiola LMD, Más BA, Duek EAR, Felisberti MI. Amphiphilic multiblock copolymers of PLLA, PEO and PPO blocks: Synthesis, properties and cell affinity. Eur Polym J [Internet]. Elsevier Ltd; 2015 Jul;68:618–29. Available from: http://dx.doi.org/10.1016/j.eurpolymj.2015.03.034

4. Kricheldorf HR, Meier-Haack J. Polylactones, 22a) ABA triblock copolymers of L-lactide and poly(ethylene glycol). Makromol Chem. 1993;194:715–25.

5. Kimura Y, Matsuzaki Y, Yamane H, Kitao T. Preparation of block copoly(ester-

ether) comprising poly(L-lactide) and poly(oxypropylene) and degradation of its fibre in vitro and in vivo. Polymer (Guildf). 1989;30:1342–9.

6. Wu X, El Ghzaoui A, Li S. Anisotropic self-assembling micelles prepared by the direct dissolution of PLA/PEG block copolymers with a high PEG fraction. Langmuir [Internet]. 2011 Jul 5;27(13):8000–8. Available from: http://www.ncbi.nlm.nih.gov/pubmed/21639089

7. Thammawong C, Buchatip S, Petchsuk A, Tangboriboonrat P, Chanunpanich N, Opaprakasit M, et al. Electrospinning of poly(l-lactide- co -dl-lactide) copolymers: Effect of chemical structures and spinning conditions. Polym Eng Sci [Internet]. 2014 Feb;54(2):472–80. Available from: http://doi.wiley.com/10.1002/pen.20921

8. Xu F, Sun LX, Tan ZC, Liang JG, Zhang T. Adiabatic calorimetry and thermal analysis on acetaminophen. J Therm Anal Calorim [Internet]. 2006 Feb 3;83(1):187–91. Available from: http://link.springer.com/10.1007/s10973-005-6969-0

9. Kauffman JF, Batykefer LM, Tuschel DD. Raman detected differential scanning calorimetry of polymorphic transformations in acetaminophen. J Pharm Biomed Anal [Internet]. 2008 Dec 15 [cited 2014 Nov 25];48(5):1310–5. Available from: http://www.ncbi.nlm.nih.gov/pubmed/18930622

10. Andrews GP, Abu-Diak O, Kusmanto F, Hornsby P, Hui Z, Jones DS. Physicochemical characterization and drug-release properties of celecoxib hot-melt extruded glass solutions. J Pharm Pharmacol [Internet]. 2010 Nov 11 [cited 2014 Nov 23];62(11):1580–90. Available from: http://doi.wiley.com/10.1111/j.2042-7158.2010.01177.x

11. Lu GW, Hawley M, Smith M, Geiger BM, Pfund W. Characterization of a novel polymorphic form of celecoxib. J Pharm Sci [Internet]. 2006 Feb [cited 2014 Nov 25];95(2):305–17. Available from: http://www.ncbi.nlm.nih.gov/pubmed/16369929

12. Łuczak A, Jallo LJ, Dave RN, Iqbal Z. Polymorph stabilization in processed acetaminophen powders. Powder Technol [Internet]. 2013 Feb [cited 2014 Nov 25];236:52–62. Available from: http://linkinghub.elsevier.com/retrieve/pii/S0032591012003737

13. Guo C, Liu H, Wang J, Chen J. Conformational Structure of Triblock Copolymers by FT-Raman and FTIR Spectroscopy. J Colloid Interface Sci [Internet]. 1999 Jan 15;209(2):368–73. Available from: http://www.ncbi.nlm.nih.gov/pubmed/9885264

14. Kang S, Hsu SL, Stidham HD, Smith PB, Leugers MA, Yang X. A Spectroscopic Analysis of Poly(lactic acid) Structure. Macromolecules [Internet]. 2001 Jun;34(13):4542–8. Available from: http://pubs.acs.org/doi/abs/10.1021/ma0016026

15. Kister G, Cassanas G, Vert M. Effects of morphology, conformation and configuration on the IR and Raman spectra of various poly(lactic acid)s. Polymer (Guildf) [Internet]. 1998 Jan;39(2):267–73. Available from: http://linkinghub.elsevier.com/retrieve/pii/S0032386197002292

16. Aou K, Hsu SL. Trichroic vibrational analysis on the α-form of poly(lactic acid) crystals using highly oriented fibers and spherulites. Macromolecules. 2006;39(9):3337–44.